Available online at www.sciencedirect.com
ScienceDirect
Biochimica et Biophysica Acta 1767 (2007) 281–294
Biochimica et Biophysica Acta BBA
www.elsevier.com/locate/bbabio

Phosphoenolpyruvate metabolism in Jerusalem artichoke mitochondria

Lidia de Bari [a,1], Daniela Valenti [a,1], Roberto Pizzuto [b], Anna Atlante [a], Salvatore Passarella [b,*]

[a] *Istituto di Biomembrane e Bioenergetica, CNR, Via G. Amendola 165/A, 70126, Bari, Italy*
[b] *Dipartimento di Scienze della Salute, Università del Molise, Via De Sanctis, 86100, Campobasso, Italy*

Received 18 September 2006; received in revised form 17 January 2007; accepted 5 February 2007
Available online 23 February 2007

Abstract

We report here initial studies on phosphoenolpyruvate metabolism in coupled mitochondria isolated from Jerusalem artichoke tubers. It was found that:

(1) phosphoenolpyruvate can be metabolized by Jerusalem artichoke mitochondria by virtue of the presence of the mitochondrial pyruvate kinase, shown both immunologically and functionally, located in the inner mitochondrial compartments and distinct from the cytosolic pyruvate kinase as shown by the different pH and inhibition profiles.
(2) Jerusalem artichoke mitochondria can take up externally added phosphoenolpyruvate in a proton compensated manner, in a carrier-mediated process which was investigated by measuring fluorimetrically the oxidation of intramitochondrial pyridine nucleotide which occurs as a result of phosphoenolpyruvate uptake and alternative oxidase activation.
(3) The addition of phosphoenolpyruvate causes pyruvate and ATP production, as monitored via HPLC, with their efflux into the extramitochondrial phase investigated fluorimetrically. Such an efflux occurs via the putative phosphoenolpyruvate/pyruvate and phosphoenolpyruvate/ATP antiporters, which differ from each other and from the pyruvate and the adenine nucleotide carriers, in the light of the different sensitivity to non-penetrant compounds. These carriers were shown to regulate the rate of efflux of both pyruvate and ATP. The appearance of citrate and oxaloacetate outside mitochondria was also found as a result of phosphoenolpyruvate addition.

Keywords: Phosphoenolpyruvate; Jerusalem artichoke mitochondria; Pyruvate kinase; Mitochondrial transport

1. Introduction

One of the most outstanding problems in plant bioenergetics concerns the fuelling of mitochondria in plant cells oxidizing carbohydrate. In addition to that metabolized in the methylglyoxal pathway which results in the formation of D-lactate [1,2], glucose is also converted by glycolysis to phosphoenolpyruvate (PEP) and finally to pyruvate via the cytosolic pyruvate kinase. Pyruvate kinase (PK) is an important regulatory enzyme of glycolysis that catalyzes the irreversible substrate level phosphorylation of ADP at the expense of PEP, yielding pyruvate and ATP. Plant PK is a primary site of control of glycolytic flux for pyruvate [3]. On the other hand, several conditions including high cytosolic energy charge [4,5], the presence of negative modulators such as glutamate [6–10] and citrate [11] and the decline in phosphate and ADP [12] cellular concentrations can severely limit PK activity thus causing PEP

Abbreviations: ADK, adenylate kinase; AOX, alternative oxidase; ALA, alanine; Ap5A, P1,P5-di(adenosine-5′)pentaphosphate; ARS, arsenite; ATP D.S., ATP detecting system; BEMA, benzylmalonate; BF, bathophenthroline; BSA, bovine serum albumin; BTA, benzentricarboxylic acid; BUMA, butylmalonate; CF, cytosolic fraction; CAT, carboxyatractyloside; CN^-, potassium cyanide; COX, cytochrome oxidase; α-CCN^-, α-cyano-4-hydroxycinnamate; DPI, diphenyleneiodonium chloride; G6PDH, glucose-6-phosphate dehydrogenase; FCCP, carbonyl cyanide 4-trifluoromethoxyphenylhydrazone; G6PDH, glucose-6-phosphate dehydrogenase; HK, hexokinase; JAM, Jerusalem artichoke mitochondria; L-LDH, L-lactate dehydrogenase; ME, malic enzyme; OLIGO, oligomycin; OXA, oxalate; OAA, oxaloacetate; P.D.S., pyruvate detecting system; PEP, phosphoenolpyruvate; PEPC, phosphoenolpyruvate carboxylase; PhePYR, phenylpyruvate; Propyl-GALL, propyl gallate; PK, pyruvate kinase; ROT, rotenone; SD, standard deviation; SHAM, salicylhydroxamic acid; TX-100, Triton X-100; TX-JAM, JAM solubilized with TX-100

* Corresponding author. Tel.: +39 080 5443364 to 65; fax: +39 080 5443317.
E-mail address: passarel@unimol.it (S. Passarella).
[1] These authors contributed equally to this work.

0005-2728/$ - see front matter © 2007 Elsevier B.V. All rights reserved.
doi:10.1016/j.bbabio.2007.02.010

accumulation in the cytosol. An additional pathway has been considered to compensate for limited pyruvate formation and transport across the mitochondrial membrane [13,14]; in this pathway, pyruvate enters mitochondria in form of malate following the combined action of the cytosolic phosphoenolpyruvate carboxylase (PEPC) and malate dehydrogenase, malate translocators and mitochondrial malic enzyme (ME) (see Scheme 1) [13,15–17].

Since it was found that all glycolytic enzymes are functionally associated with mitochondria from Arabidopsis, the possibility that mitochondria possess their own PK should be taken in consideration. In this regard, PK was reported to have one isoform predicted to be targeted to mitochondria [18]. Consistently, a gene search for PK in TAIR database (Arabidopsis Information Resource) identified two matches (AT3G25960 and AT3G55810) which correspond to isoforms predicted by Target P program to be targeted to mitochondria.

All together the above considerations show that the interaction between glycolysis intermediates and energy metabolism in mitochondria is far from being established. In particular, the capability of glycolytic compounds including PEP to enter and to be metabolized in the mitochondria is far from being elucidated.

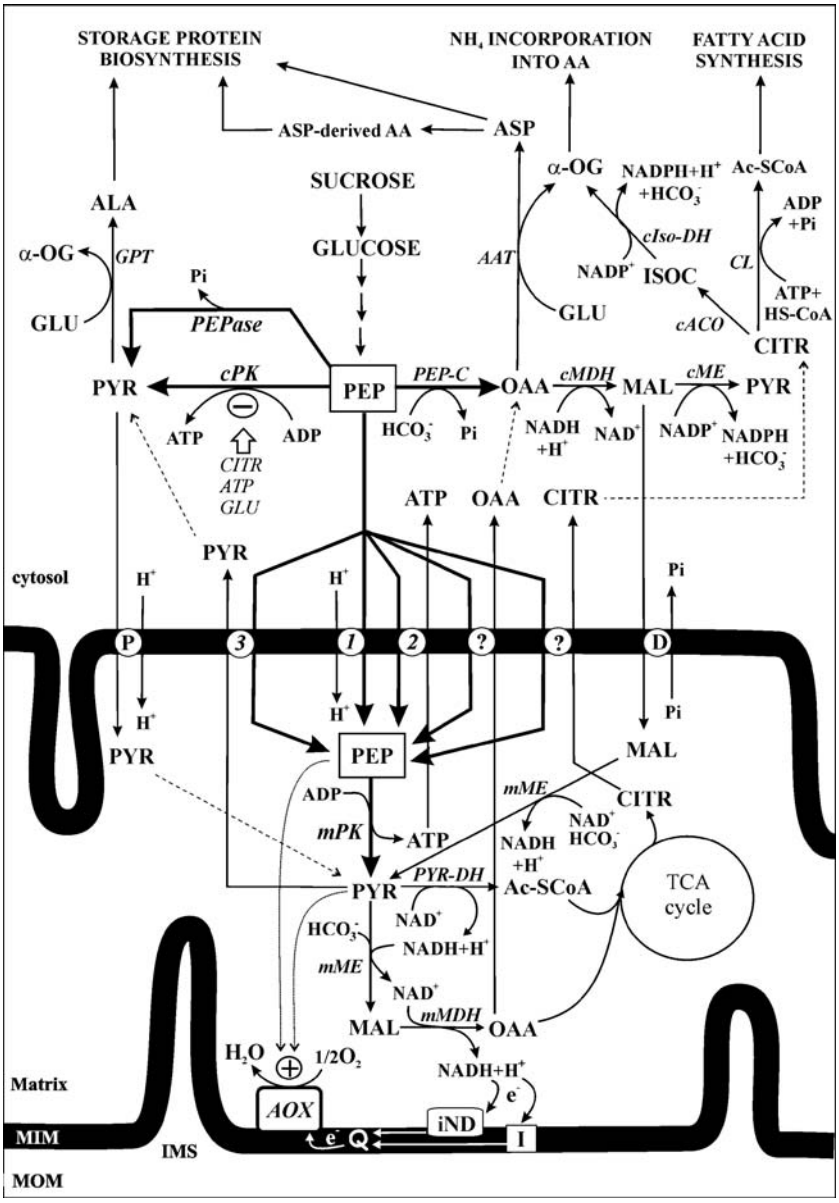

Scheme 1. PEP transport and metabolism in JAM. For explanation see the text. Abbreviations used in the figure: PEP, phosphoenolpyruvate; PYR, pyruvate; ALA, alanine; OAA, oxaloacetate; MAL, malate; CITR, citrate; ISOC, isocitrate; HS-CoA, coenzyme A; Ac-SCoA, acetyl-SCoA; GLU, glutamate; ASP, aspartate; α-OG, α-oxoglutarate; Pi, inorganic phosphate; MIM, mitochondrial inner membrane; MOM, mitochondrial outer membrane; IMS, intermembrane space; enzymes: cPK, mPK, cytosolic, mitochondrial pyruvate kinase; mMDH, cMDH, cytosolic, mitochondrial malate dehydrogenase; PEPase, phosphoenolpyruvate phosphatase; PEP-C, phosphoenolpyruvate carboxylase; cME, mME, cytosolic, mitochondrial malic enzyme; PYR-DH, pyruvate dehydrogenase complex; GPT, glutamate pyruvate transaminase; AAT, aspartate amino transaminase; cACO, cytosolic aconitase; cIso-DH, cytosolic isocitrate dehydrogenase; CL, citrate lyase; iND, internal NAD(P)H dehydrogenase; I, complex I of the respiratory chain; Q, coenzyme Q; AOX, alternative oxidase; carriers: ***1***, PEP/H+ symporter; ***2***, PEP/ATP antiporter; ***3***, PEP/PYR antiporter; ***P***, pyruvate carrier; ***D***, dicarboxylate carrier; **?**, PEP transporters.

Here we investigate whether and how mitochondria from Jerusalem artichoke, used as a model system, can metabolize externally added PEP, perhaps triggering a novel mitochondrion–cytosol crosstalk. We report both immunological and functional evidence of the existence of a mitochondrial PK which charges mitochondria with pyruvate and ATP thus promoting novel metabolite traffic across the mitochondrial membranes and which may be involved in cytosolic biosynthetic processes. Interestingly, PEP appears to be a novel alternative oxidase activator.

2. Materials and methods

2.1. Materials

All reagents were from SIGMA with the exception of sucrose, Triton X-100, HEPES, Tris and sodium arsenite (Baker).

All chemicals were of purest grade available and were used as Tris salts at pH 7.0–7.4 adjusted with Tris or HCl. Rotenone, oligomycin and FCCP were dissolved in ethanol.

Jerusalem artichoke tubers were kindly supplied by Prof. A. De Santis (Università Politecnica delle Marche).

2.2. Isolation of JAM and preparation of the cytosolic fraction

Jerusalem artichoke mitochondria (JAM) were isolated as in [19] and checked for their intactness [20,21]. Mitochondria showing intactness lower than 90 and 95% for the outer and inner membranes respectively were discarded. Mitochondrial coupling was also checked: JAM showed respiratory control equal to 2.6±0.24 as in [22].

The cytosolic fraction (CF) was obtained by centrifuging (105,000×g for 60 min at 4 °C) the supernatant obtained during isolation of JAM. Glucose-6-phosphate dehydrogenase (G6PDH) (E.C. 1.1.1.49) and adenylate kinase (ADK) (E.C. 2.7.4.3.), cytosolic and mitochondrial markers, respectively, were assayed as in [23] and [24].

2.3. Immunoblot analysis

Immunoblot analysis was performed on either total mitochondrial or total cytosolic protein by using antibodies raised against PK and β-tubulin. Polyclonal antibody recognizing β-tubulin was used as a marker of cytosol.

Both JAM and CF were solubilized in Triton X-100 (TX-100, 1%), 500 mM NaCl, 50 mM Tris–HCl pH 7.5, 1 mM EGTA, 1 mM EDTA, 0.5 mM dithiothreitol, 0.1 mM PMSF for 30 min on ice. Protein content was determined using the Bradford reagent (Bio-Rad Laboratories) with bovine serum albumin (BSA) as a standard. Both mitochondrial and cytosolic solubilized proteins (40 μg each) were subjected to electrophoresis on 12% SDS-polyacrylamide gel [25]. Following electrophoresis, protein blots were transferred to a PVDF membrane. The membrane was blocked with 5% non-fat milk in TBS solution, and incubated overnight with the corresponding primary antibodies in the blocking solution at 4 °C. After washing three times with TBS-T solution (0.3%), the membrane was incubated at room temperature for 1 h with HRP-conjugated secondary antibody. The detected protein signals were visualized by using the Enhanced Chemiluminescence Western Blotting reagents (Amersham).

2.4. Pyruvate kinase assay

Because the external mitochondrial NAD(P)H dehydrogenase rapidly oxidizes NADH used in the PK assay via L-lactate dehydrogenase (L-LDH), PK activity was mostly monitored by measuring the rate of ATP formation, revealed by using the ATP detecting system (ATP D.S.) consisting of glucose (2.5 mM), hexokinase (HK, 0.5 e.u.), G6PDH (0.5 e.u.) and $NADP^+$ (0.2 mM). The detection was done fluorimetrically at the excitation-emission wavelengths of 334–456 nm as in [26,27] using a Perkin Elmer LS-50 luminometer, with the NAD(P)H fluorescence calibrated as described in [28–30]. Briefly, either the cytosol fraction (0.2 mg of cytosol protein) or JAM (0.5 mg of mitochondrial protein), in the absence or presence of TX-100 (0.2%), was incubated at 25 °C in 2 mL of standard medium consisting of 0.29 mM sucrose, 20 mM KCl, 20 mM HEPES–Tris pH 7.0, 10 mM $MgCl_2$, in the presence of ATP D.S. Where indicated, 0.1 mM P1,P5-di(adenosine-5′) pentaphosphate (Ap5A), a specific inhibitor of ADK [31] was also added. The reaction was started by the addition of either PEP or ADP at the concentrations reported in the legends of the relevant figures, in the presence of 0.25 mM ADP or 5 mM PEP, respectively. The rate of $NADP^+$ reduction was followed as fluorescence increase and measured as the tangent to the initial part of the progress curve. The specific activity was expressed as nmol $NADP^+$ reduced/min × mg cytosol or mitochondrial protein. Control experiments confirmed that none of the compounds used in this paper affects the enzymes used to reveal pyruvate kinase activity.

When pyruvate production was measured (as in [4]) NADH (0.1 mM) plus L-lactate dehydrogenase (L-LDH) (1 e.u.) were used in the presence of EGTA (10 mM) plus diphenyleneiodonium (DPI, 5 μM) and rotenone (ROT, 2 μg), used to inhibit oxidation of externally added NADH by JAM. The rate of NADH oxidation by pyruvate was corrected for the spontaneous NADH oxidation by JAM.

2.5. Swelling experiments

Mitochondrial swelling was followed at 25 °C at 546 nm using a Perkin-Elmer Lambda-5 spectrophotometer. JAM (1 mg protein) were rapidly added to 1.5 mL of isotonic solutions of ammonia salts whose pH was adjusted to 7.2, and the decrease in the absorbance continuously recorded.

2.6. Fluorimetric and photometric assays

Changes in the redox state of mitochondrial pyridine nucleotides were monitored fluorimetrically, using a Perkin Elmer luminometer LS-50 with excitation–emission wavelengths of 334–456 nm. The NAD(P)H fluorescence was calibrated as in [28–30]. JAM (1 mg protein) were incubated in 2 mL of standard medium and the fluorescence changes monitored as a function of time.

PEP uptake was monitored by measuring the intramitochondrial NAD(P)H oxidation caused by externally adding the substrate to JAM.

ATP, pyruvate, oxaloacetate (OAA) and citrate appearance outside mitochondria was monitored by using the ATP D.S. in the presence of Ap5A (0.1 mM) and succinate (5 mM) used to energize mitochondria, the pyruvate detecting system (P.D.S.) consisting of 20 μM NADH plus L-LDH (1 e.u.), the oxaloacetate detecting system (O.D.S.) consisting of 20 μM NADH plus malate dehydrogenase (1 e.u.) and the citrate detecting system (C.D.S.) consisting of O.D.S. plus citrate lyase (1 e.u.), ATP (1 mM) and coenzyme A (1 mM). When either pyruvate, oxaloacetate or citrate efflux was monitored, JAM were pre-incubated in the presence of EGTA (10 mM) plus diphenyleneiodonium chloride (DPI) (5 μM) and ROT (2 μg), used to prevent oxidation of externally added NADH by both the external mitochondrial NAD(P)H dehydrogenase and complex I of respiratory chain, respectively. The decreased NADH concentration (20 μM instead of 0.1 mM) used to reveal pyruvate appearance outside intact mitochondria was necessary to prevent NADH oxidation by external NADH-DH which was not completely inhibited by the presence of rotenone/EGTA/DPI. It was established that under these conditions the activity of the P.D.S. was not limiting in determining the rate of pyruvate production.

The reduction of $NADP^+$ in the case of ATP, or the oxidation of NADH in the case of either pyruvate, oxaloacetate or citrate, consequent on PEP addition to JAM, was followed as either fluorescence increase or decrease, measured as the tangent to the initial part of the progress curve and expressed as nmol $NADP^+$ reduced (NADH oxidized)/min × mg mitochondrial protein, respectively. Citrate appearance rate was calculated by subtracting the rate of oxaloacetate appearance from the rate of absorbance decrease found in the presence of the C.D.S. In the case of ADP/ATP carrier measurement, ADP was added to JAM at the concentrations reported in the relevant Figs, under the same experimental conditions used for the detection of PEP-dependent ATP efflux.

Malate appearance was monitored photometrically as in [2] by following the absorbance increase at the wavelength of 334 nm in the presence of the malate

detecting system (M.D.S.) consisting of 200 μM $NADP^+$ plus malic enzyme (ME, 0.2 u.e). The value of ε_{334} measured for NAD(P)H under our experimental conditions was found to be 6.22 mM^{-1} cm^{-1}.

PEP *per se* proved to have no effect on the enzymatic reactions or on either the absorbance or the fluorescence measured. Moreover, controls were carried out to ensure that none of the compounds used affected the enzymes used to reveal metabolite appearance outside mitochondria.

2.7. HPLC measurements

All the measurements were carried out by means of a Kontron Instrument HPLC system including a model 420 pump and a model 425 gradient former equipped with a data system 450 MT2. In a typical experiment, JAM (1 mg protein) were incubated for 1 min in 1 mL of standard medium plus 0.1 mM Ap_5A and then PEP (5 mM) was added either in the absence or presence of oligomycin (OLIGO, 2.5 μg/mL). After 1 min of incubation the suspension was rapidly centrifuged for 1 min at 13000 rpm in a refrigerated Eppendorf microcentrifuge. Perchloric acid extracts of both supernatant and pellet were obtained and neutralized as in [32]. In order to determine the amount of ADP and ATP, aliquots of the neutralized perchloric acid extracts were analyzed by means of HPLC as previously reported [33], with a calibration made in each experiment.

3. Results

3.1. The occurrence of pyruvate kinase activity in solubilized mitochondria from Jerusalem artichoke tubers

In order to ascertain whether JAM can metabolize externally added PEP, first we investigated the occurrence of PK in coupled JAM (Fig. 1A). An immunological analysis carried out by using anti-PK antibodies showed the occurrence of the mitochondrial PK. Each mitochondrial sample was also subjected to Western blotting for β-tubulin, as a cytosolic marker, using a polyclonal anti-β-tubulin antibody; JAM were found to be completely free of cytosolic contamination since no β-tubulin was detected. The immunological analysis of the cytosolic fraction of the same preparation, used as a control, showed the presence of both cytosolic PK and β-tubulin.

The existence of a putative mitochondrial PK protein was confirmed by measurement of the reaction catalyzed by PK in

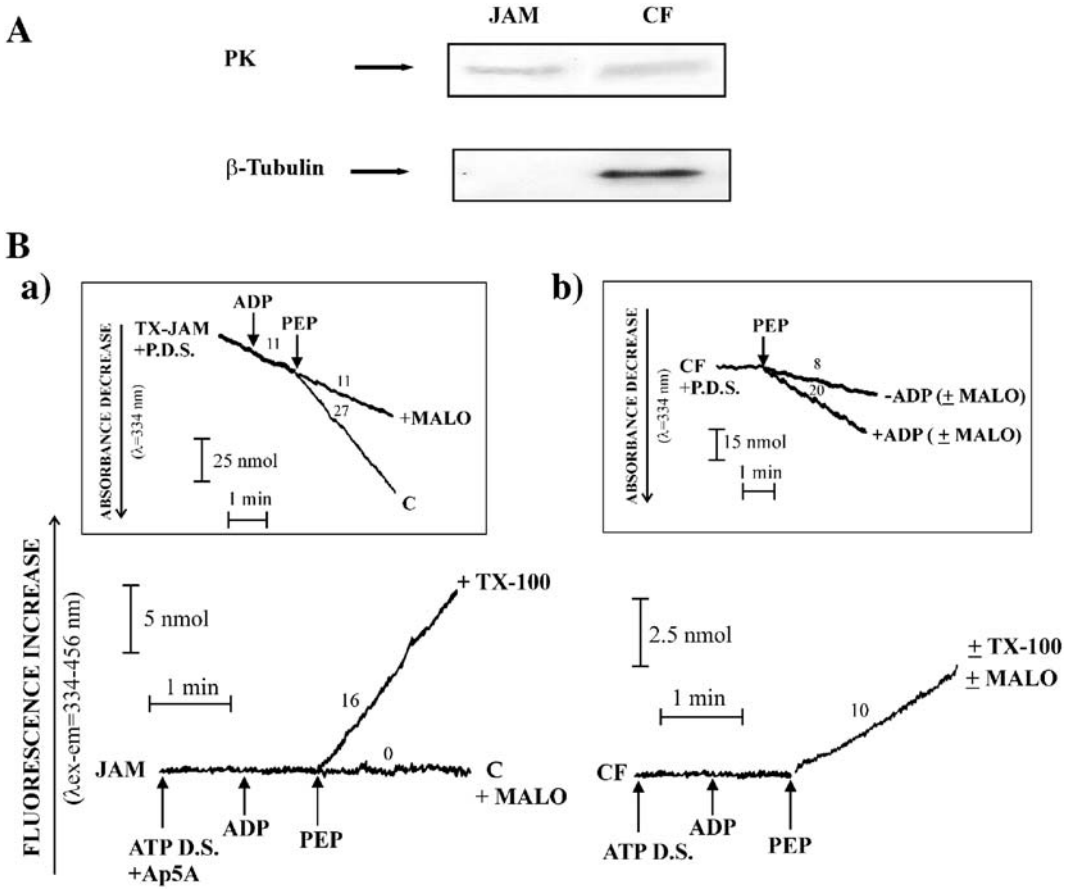

Fig. 1. Immunodetection of mitochondrial PK and pyruvate kinase activity assay in JAM and CF. (A) Solubilized proteins from both JAM and CF (40 μg each) were analyzed by Western blotting as described in Materials and methods. Membrane blots were incubated with polyclonal anti-PK and anti-β-tubulin antibodies. β-tubulin was used as a cytosolic marker. (B) Either JAM (0.5 mg mitochondrial protein) (a) or CF (0.2 mg protein) (b) were incubated at 25 °C in the absence (C) or presence of the detergent TX-100 (0.2%) in 2 mL of standard medium in the presence of ATP D.S. When indicated, 0.1 mM Ap5A was also present (a). At the arrow, ADP (0.25 mM) and PEP (5 mM) were added. Where indicated, MALO (10 mM) was added 1 min before the substrates to either JAM solubilized with TX-100 or CF either in the absence or presence of the detergent. PK activity was monitored fluorimetrically at the excitation–emission wavelength of 334–456 nm (see Materials and methods). Numbers along curves are rates of fluorescence increase measured as the tangents to the initial part of the progress curve and expressed as nmol $NADP^+$ reduced/min × mg of sample protein. Insets report either TX-JAM (1 mg protein, inset a) or CF (1 mg protein, inset b) incubated at 25 °C in 2 mL of standard medium in the presence of P.D.S. When indicated, ADP (0.25 mM) was also present. At the arrow, PEP (5 mM) was added. Where indicated, MALO (10 mM) was added 1 min before PEP addition to either TX-JAM or CF. PK activity was monitored photometrically at 334 nm (see Materials and methods). Numbers along curves are rates of absorbance decrease measured as the tangents to the initial part of the progress curve and expressed as nmol NADH oxidized/min × mg of sample protein.

isolated JAM (Fig. 1B) and the kinetics of the process were examined. This was done fluorimetrically, by measuring the pyridine nucleotide fluorescence increase, which occurs as a result of appearance of ATP (one of the product of the PK reaction) as detected by the presence of glucose, HK, G6PDH and $NADP^+$ (the ATP D.S.) plus 0.25 mM ADP and 0.1 mM Ap5A, used to inhibit ADK [31] (Fig. 1B, a). The CF of the same preparation was used as a control, but in this case no Ap5A was present (Fig. 1B, b). ATP concentration outside intact JAM (0.5 mg mitochondrial protein) and in the CF (0.2 mg cytosol protein) was negligible since no fluorescence change was found in the presence of ATP D.S. No increase in NADPH fluorescence was found when ADP (0.25 mM) was added, this showing the complete inhibition of ADK activity in the mitochondrial preparation (Fig. 1B, a). As a result of PEP addition to intact JAM no significant fluorescence change was found, this indicating the absence of PK in the outer membrane, in the intermembrane space or on the outer side of the mitochondrial inner membrane and excluding any contamination of the mitochondrial fraction with the cytosolic PK (Fig. 1B, a). In a control experiment, no G6PDH activity, measured as in [23], was found either in intact or solubilized JAM thus further confirming the absence of cytosolic contamination; conversely, no ADK activity, a mitochondrial inter-membrane space marker, measured as in [24], was found in the CF, thus excluding both the presence of mitochondrial contamination and of mitochondrial outer membrane rupture (Fig. 1B, b).

Surprisingly enough, when the membrane detergent Triton X-100 (TX-100, 0.2%) was added to JAM (0.5 mg mitochondrial protein) in order to dissolve the mitochondrial membranes, NADPH formation was found following PEP (5 mM) addition with a rate of 16 nmol $NADP^+$ reduced/min × mg of mitochondrial protein (Fig. 1B, a). As expected, an increase in NADPH fluorescence was observed when PEP (5 mM) was added to the CF, reflecting the activity of the cytosolic PK and found to be equal to 10 nmol $NADP^+$ reduced /min × mg of cytosol protein both in the absence and presence of TX-100 (0.2%) (Fig. 1B, b). Interestingly, in distinction with the CF, no fluorescence increase was found when JAM solubilized with 0.2% TX- 100 (TX-JAM) were incubated with malonate (MALO, 10 mM) for 1 min before PEP addition. (Fig. 1B, a and b). As expected, no PK activity was measured when both mitochondrial and cytosolic samples were boiled to denaturate the proteins (not shown). In agreement with the above findings, as a result of the addition of PEP to TX-JAM (1 mg mitochondrial protein), pyruvate formation was found occurring at the same rate as that of ATP production, and was completely prevented by MALO (10 mM) (inset to Fig. 1B, a). Pyruvate formation, as checked in CF, was not sensitive to MALO, either in the absence or presence of ADP (inset to Fig. 1B, b).

The dependence of the rate of $NADP^+$ reduction on increasing PEP (at 0.25 mM ADP) (Fig. 2A) or ADP concentrations (at 5 mM PEP) (Fig. 2B) was investigated in TX-JAM (●) and in CF (○). In both cases saturation characteristics were found with K_m(PEP) values of 200 and 500 μM and K_m(ADP) values of 60 and 40 μM, for TX-JAM and CF, respectively; V_{max} values were of 16 and 12 nmol/min × mg of sample protein, respectively, with both substrates. In three experiments, carried out with different TX-JAM and CF preparations, the mean K_m(PEP) values were found to be 200 ± 20 μM and 500 ± 20 μM, whereas the mean K_m(ADP) values were found to be 60 ± 5 μM and 40 ± 4 μM, for the mitochondrial and cytosolic PK, respectively. In the same experiments, the mean V_{max} values were 16 ± 1 and 13 ± 2 nmol/min × mg of sample protein for the mitochondrial and cytosolic PK, respectively.

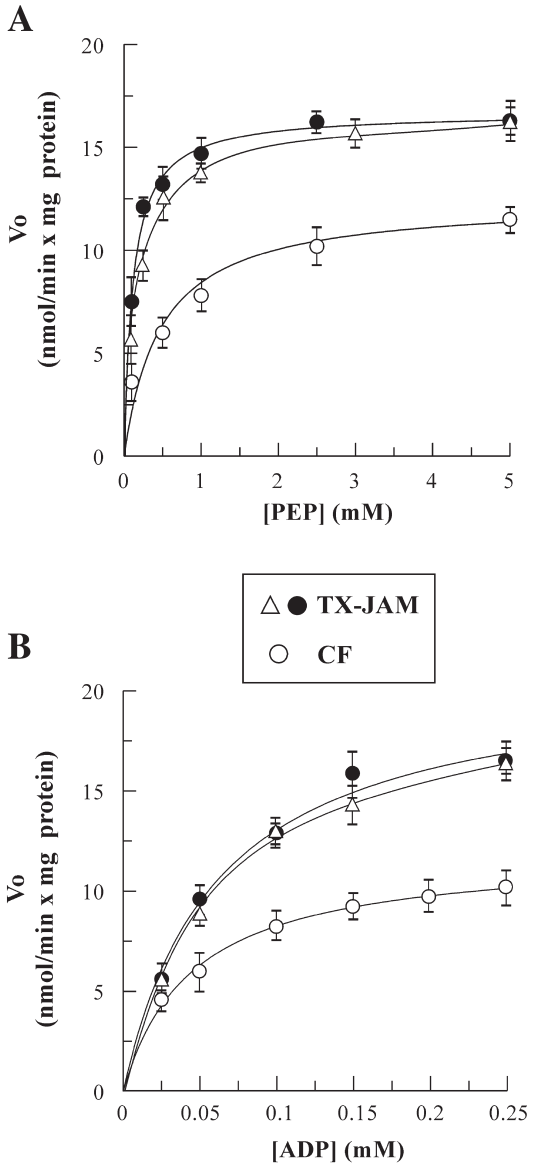

Fig. 2. The dependence of ATP and pyruvate appearance on increasing concentrations of either PEP or ADP. (A) PEP at 0.25 mM ADP, or (B) ADP at 5 mM PEP, were added at the indicated concentrations to either TX-JAM (0.5 mg mitochondrial protein) (Δ, ●) or CF (0.2 mg cytosol protein) (○) and either ATP (●, ○) or pyruvate (Δ) appearance was investigated as described in Materials and methods. The rate (V_o) of $NADP^+$ reduction (●, ○) or NADH oxidation (Δ) was calculated as the tangent to the initial part of the progress curve and expressed as nmol/min × mg of sample protein. Bars represent the mean (± SD) of three independent measurements.

In the case of the TX-JAM, the PK reaction was also investigated by measuring the pyruvate formation via L-LDH

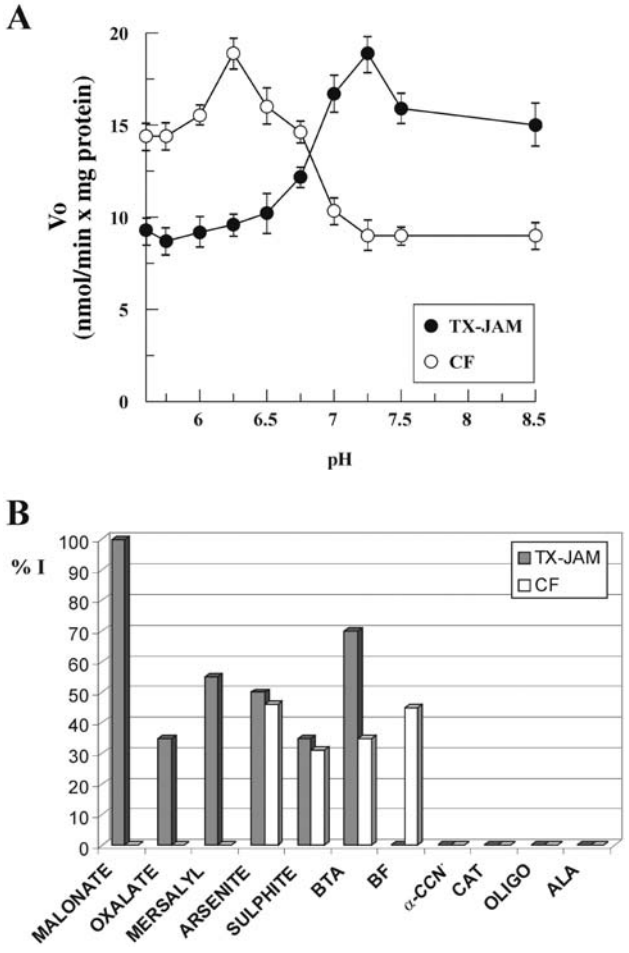

Fig. 3. pH profiles and the sensitivity to a variety of compounds of mitochondrial and cytosolic pyruvate kinase activity. (A) Either TX-JAM (0.5 mg protein, ●) or CF (0.2 mg protein, ○) were incubated at 25 °C in 2 mL of standard medium whose pH was adjusted to the indicated values with either TRIS or HCl. Experimental conditions as in Fig. 1. PEP and ADP concentration used were 5 and 0.25 mM, respectively. Bars represent the mean (±SD) of three independent measurements. (B) PK activity was measured as described in Fig. 1, by adding 0.1 mM PEP to either TX-JAM (0.5 mg protein) or CF (0.2 mg protein) incubated at 25 °C in 2 mL of standard medium in the presence of 0.25 mM ADP, either in the absence or presence of the following compounds (added to the sample 1 min before the substrate): malonate (10 mM), oxalate (10 mM), mersalyl (0.1 mM), arsenite (1 mM), sulphite (2 mM), benzentricarboxylic acid (BTA, 1 mM), bathophenanthroline (BF, 0.1 mM), α-CCN$^-$ (1 mM), CAT (10 μM), oligomycin (OLIGO, 5 μM) and alanine (ALA, 5 mM).

assay (Δ, Figs. 2A, B). The K_m and V_{max} values were essentially similar to those determined using the alternative assay described above.

In order to confirm that the above reactions were catalyzed by two different PKs, the pH and inhibition profiles of PK from either mitochondrial or cytosol fraction were also investigated fluorimetrically as above, with 5 mM PEP and 0.25 mM ADP (Fig. 3A). The pH profiles differ one from another significantly: PK activity in solubilized JAM was found to increase with pH increase, reaching its maximum value over the pH range 7.00–8.50, whereas when CF was used the maximum activity was found at pH 6.25. The activity decreased at pH values over 6.75. In both cases PK activities were roughly constant in the pH range 7.5–8.5.

The mitochondrial and cytosolic PK reactions, monitored at 0.1 mM PEP and 0.25 mM ADP, were also compared with respect to their sensitivity to a variety of compounds, including MALO (10 mM), oxalate (10 mM), arsenite (1 mM), sulphite (2 mM), inhibitors of succinate, lactate, pyruvate and malate dehydrogenase respectively. The thiol reagent mersalyl (0.1 mM), benzentricarboxylic acid (BTA, 1 mM), the metal complexing agent bathophenanthroline (BF, 0.1 mM), α-cyano-4-hydroxycinnamate (α-CCN-, 1 mM) carboxyatractyloside (CAT, 10 μM), inhibitors of some mitochondrial carriers [34,35], OLIGO (5 μM), an inhibitor of ATP synthase and alanine (ALA, 5 mM) were also used (Fig. 3B). The inhibition profiles proved to differ significantly one from another. For instance, MALO, oxalate or mersalyl proved to inhibit specifically the mitochondrial PK, whereas BF, which was ineffective on the mitochondrial PK, inhibited by 45% the cytosolic enzyme.

3.2. PEP transport in JAM

Having established that JAM possess their own PK, located in the inner mitochondrial compartments, we investigated whether and how externally added PEP can enter mitochondria. As an initial approach to this problem, swelling experiments were carried out as in [36] (Fig. 4A). Intact coupled JAM suspended in 0.14 M ammonium PEP showed spontaneous swelling, at a rate lower than that found for 0.14 M ammonium phosphate (NH_4P_i), used as a control, this suggesting the capability of PEP to enter JAM itself, in a proton-compensated manner. The rate of JAM swelling in the isotonic ammonium PEP solution proved to be inhibited in the presence of the non-penetrant compound benzylmalonate (BEMA, 10 mM), this suggesting that the uptake occurs in a carrier mediated manner. As a control, it was confirmed that JAM do not swell in isotonic sucrose solutions (Fig. 4A). In order to better investigate PEP transport in JAM, by using substrate concentrations close to physiological values, we resorted to a spectroscopic technique which allows for measurement in organelles in which metabolism is largely occurring. Thus, the capability of externally added PEP to affect the red/ox state of the intramitochondrial pyridine coenzymes was checked by means of fluorimetric techniques, essentially as in [1] (Fig. 4B). Surprisingly, a decrease of fluorescence was found as a result of PEP (1 mM) addition to JAM (0.5 mg protein), reflecting intramitochondrial NAD(P)H oxidation. Notice that no significant reduction of the mitochondrial NAD(P)$^+$ was found also as a result of PEP addition to JAM previously incubated with the uncoupler FCCP (not shown). Since plant mitochondria contain the alternative oxidase (AOX) which can oxidize the newly synthesized NAD(P)H in the non-phosphorylating alternative pathway [37], we checked whether the NAD(P)H oxidation was dependent on AOX activity, perhaps activated by PEP itself and/or by pyruvate, a powerful AOX activator [38,39], produced in the PK reaction. The initial rate of fluorescence decrease proved to be strongly inhibited by either propyl gallate (Propyl-GALL, 2 mM) or salicylhydroxamate (SHAM, 1 mM), inhibitors of the AOX [40–42] (50±4% and 30 ± 5% of the control, respectively, in three experiments

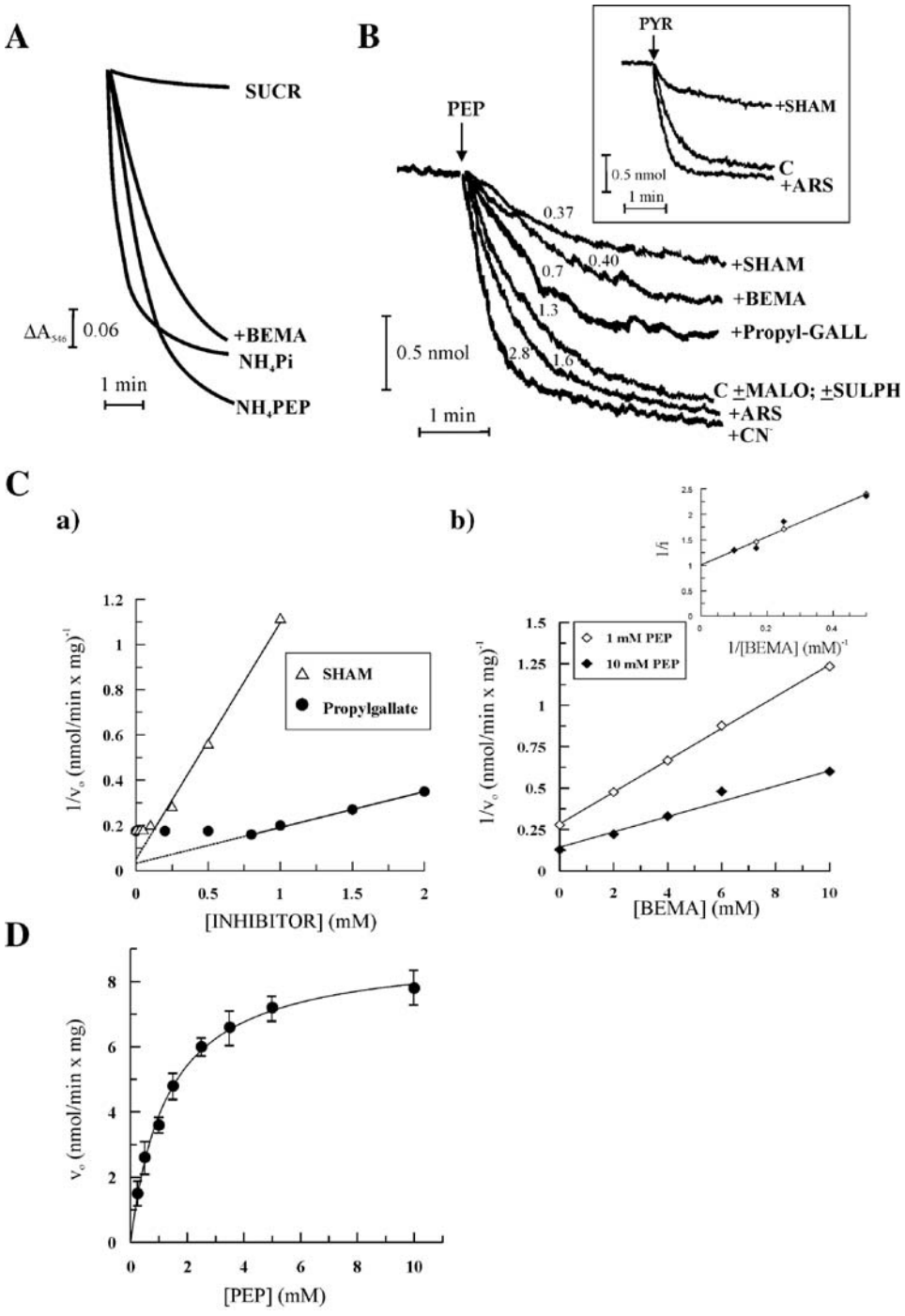

Fig. 4. Mitochondrial swelling in ammonium phosphoenolpyruvate solutions (A), fluorimetric investigation of the redox state of the intramitochondrial pyridine nucleotides (B), Dixon plot of the inhibition by either propylgallate, SHAM or BEMA (C) and the dependence of the rate of intramitochondrial pyridine nucleotides oxidation on increasing PEP concentrations (D). (A) JAM (1 mg protein) were rapidly added at 25 °C to 1.5 mL of 0.14 M ammonium phosphate (NH_4P_i), 0.36 M sucrose (SUCR), 0.14 M ammonium phosphoenolpyruvate (NH_4PEP) or 0.14 M ammonium phosphoenolpyruvate plus 10 mM benzylmalonate (BEMA) and mitochondrial swelling monitored as described in Materials and methods. The initial A_{546} nm of JAM suspended in sucrose was about 1.0. (B) JAM (0.5 mg protein) were incubated at 25 °C in 2 mL of standard medium. At the arrows, PEP (1 mM) or pyruvate (PYR, 1 mM) (inset) were added in the absence (C) or presence of the following inhibitors (added 1 min before the substrate): propyl gallate (Propyl-GALL, 2 mM), SHAM (1 mM), BEMA (10 mM), sulphite (SULPH, 2 mM), MALO (10 mM), arsenite (ARS, 1 mM) or potassium cyanide (CN^-, 1 mM). Mitochondrial pyridine nucleotide oxidation was followed fluorimetrically (λ_{exc}=334 nm; λ_{em}=456 nm) as a function of time. The numbers along the curves are rates calculated as the tangent to the initial part of the experimental trace expressed as nmol NAD(P)H oxidized/min × mg protein. (C) The rate of intramitochondrial pyridine nucleotide oxidation was measured after the addition of either 2.5 mM (a) or 1 mM and 10 mM PEP (b) to JAM (1 mg protein) either in the absence or presence of Propyl-GALL, SHAM or BEMA at the indicated concentrations. The inset in C, b is the plot of $1/i$ against 1/[BEMA], where $i = 1 - v_i/v_o$; v_i and v_o being the rate of intramitochondrial pyridine nucleotide oxidation in the presence and in the absence of inhibitor, respectively. (D) PEP was added at the indicated concentrations to JAM (1 mg protein). The rate of fluorescence decrease (v_o), was measured as the tangent to the initial part of the progress curves and expressed as nmol NAD(P)H oxidized/min × mg mitochondrial protein. Bars represent the mean (±SD) of three independent measurements.

carried our with separate mitochondrial preparations). The non-penetrant compound BEMA (10 mM) proved to inhibit the fluorescence change (35±4% of the control) which was insensitive to either sulphite (2 mM) or MALO (10 mM), whereas stimulation in intramitochondrial NAD(P)H oxidation rate was found when arsenite (ARS, 1 mM), an inhibitor of pyruvate dehydrogenase, was present (25±3% of the control). A rate of about 200±10% of the control was found in the presence of potassium cyanide (CN^-, 1 mM), an inhibitor of cytochrome oxidase (COX) (Fig. 4B). Similarly, in a control experiment, NAD(P)H fluorescence decrease was found resulting from the addition of pyruvate (1 mM), the rate being strongly inhibited by SHAM (1 mM), but stimulated by ARS (1 mM) (inset of Fig. 4B). One possible explanation of these findings is that PEP enters JAM and, subsequently, the activation of AOX occurs by PEP itself, as shown by the failure of MALO, which impairs pyruvate formation via PK, to affect the rate of fluorescence decrease, and/or by pyruvate, thus determining the cyanide-insensitive oxidation of intramitochondrial NAD(P)H.

In order to investigate whether the rate of fluorescence decrease mirrors the rate of PEP uptake by JAM, control flux analysis was carried out as in [35] (Fig. 4C). Thus, the dependence of the rate of fluorescence decrease on increasing concentrations of either Propyl-GALL or SHAM (Fig. 4C, a) at 2.5 mM PEP, or BEMA (Fig. 4C, b) at 1 mM and 10 mM PEP, was investigated in the same experiment and the data plotted as a Dixon plot. In the former case, the y intercepts of the lines fitting the experimental points obtained in the presence of the inhibitors did not coincide with the experimental values obtained in their absence, this showing that the inhibitor-sensitive step, i.e. AOX reaction, which determines intramitochondrial NAD(P)H oxidation, is not rate limiting for the measured process. Contrarily, in the presence of increasing BEMA concentrations, the y intercepts of the lines fitting the experimental points measured at both 1 and 10 mM PEP, coincided with the experimental values measured in the absence of inhibitor, as shown by the Dixon plot. In accordance with the control flux analysis [35], this shows that BEMA-sensitive PEP transport controls the rate of the measured process, i.e. the rate of NAD(P)H fluorescence decrease reflects the rate of PEP uptake by JAM. As expected in the light of the swelling inhibition (Fig. 4A), BEMA proved to be a non-competitive inhibitor of PEP uptake with a K_i value equal to 3 mM. The data of Fig. 4C, b were also plotted as 1/i against 1/[Inhibitor], where the fractional inhibition i is equal to $1-v_i/v_o$ (inset of Fig. 4C, b). The y intercept was unity, showing that BEMA can prevent PEP transport completely, thus indicating that no PEP uptake by JAM can occur either by BEMA-insensitive processes or by diffusion.

The dependence of the rate of NADH oxidation on increasing PEP concentrations was investigated in JAM and saturation characteristics were found with K_m and V_{max} values of 1.3 mM and 8.9 nmol/min × mg of protein, respectively (Fig. 4D). In three experiments, carried out with different preparations, the mean K_m and V_{max} values were found to be 1.2±0.1 mM and 10±2 nmol/min × mg of protein, respectively.

The metabolite transport paradigm (see Ref. [35]) suggests that net carbon uptake by mitochondria is accompanied by the efflux of newly synthesized compounds. In order to determine whether this applies in the case of PEP, in a first set of experiments we checked for the efflux of pyruvate and ATP, the products of the mitochondrial PK reaction, following PEP uptake and metabolism by JAM (Fig. 5). In order to detect the appearance of pyruvate in the extramitochondrial phase, JAM (1 mg protein) were incubated with ROT (2 μg/2 mL), inhibitor of complex I of the respiratory chain and with 10 mM EGTA plus 5 μM DPI, in order to inhibit the external mitochondrial NAD(P)H dehydrogenase, then the P.D.S. consisting of L-LDH (1 e.u.) and NADH (20 μM), used at low concentration in order to minimize external NAD(P)H dehydrogenase activity [43], was added to the mitochondrial suspension and NADH fluorescence measured (see Materials and methods) (Fig. 5A). As a result of PEP (5 mM) addition, a decrease in the NADH fluorescence was found, at a rate of 5.0 nmol NADH oxidized/min × mg protein, indicative of the appearance of pyruvate in the extramitochondrial phase. In the same experiment, we found that the mitochondrial PK inhibitor MALO (10 mM) completely inhibited the appearance of pyruvate, ruling out the possibility that pyruvate formation occurred via the cytosolic PEP phosphatase shown to be insensitive to MALO (inset to Fig. 1B, b).

In order to ascertain whether PEP can cause the efflux of mitochondrial ATP, JAM (1 mg protein) were incubated with 0.1 mM Ap5A and with 5 mM succinate, used to inhibit ADK and to energize mitochondria, respectively, thus favoring the membrane potential dependent ATP efflux, and ATP appearance was measured as above. ATP concentration outside mitochondria was negligible since no fluorescence increase occurred when ATP D.S. was added to the mitochondrial suspension. As a result of PEP (5 mM) addition, an increase in NADPH fluorescence was found, at a rate equal to 2.7 nmol $NADP^+$ reduced/min × mg protein, indicating the appearance of ATP in the extramitochondrial phase (Fig. 5B).

A possible explanation of these findings is that PEP, which can enter JAM itself, forms ATP and pyruvate in the matrix because of the presence of the mitochondrial PK and endogenous ADP; newly synthesized ATP and pyruvate can, in turn, get to the extramitochondrial phase in exchange with further PEP (see Scheme 1).

One could argue that ATP efflux could depend also on the presence of ADP formed outside mitochondria by the ATP D.S. when revealing ATP efflux. To gain further insight into this point as well as to ascertain whether the effluxed ATP derives from substrate level phosphorylation, we directly checked the capability of PEP to synthesize ATP from the intramitochondrial ADP, via HPLC analysis. In this case we incubated JAM with Ap5A (0.1 mM). In a typical experiment (Fig. 5C) we measured the amounts of ADP and ATP in the pellet and supernatant of a mitochondrial suspension incubated or not with 5 mM PEP. The addition of PEP to JAM, either in the absence or presence of OLIGO (2.5 μg/1 mL) used to inhibit the ATP synthase, resulted in a decrease in the mitochondrial content of both ADP and ATP [$\Delta(ADP_{IN}+ATP_{IN})$], and in the

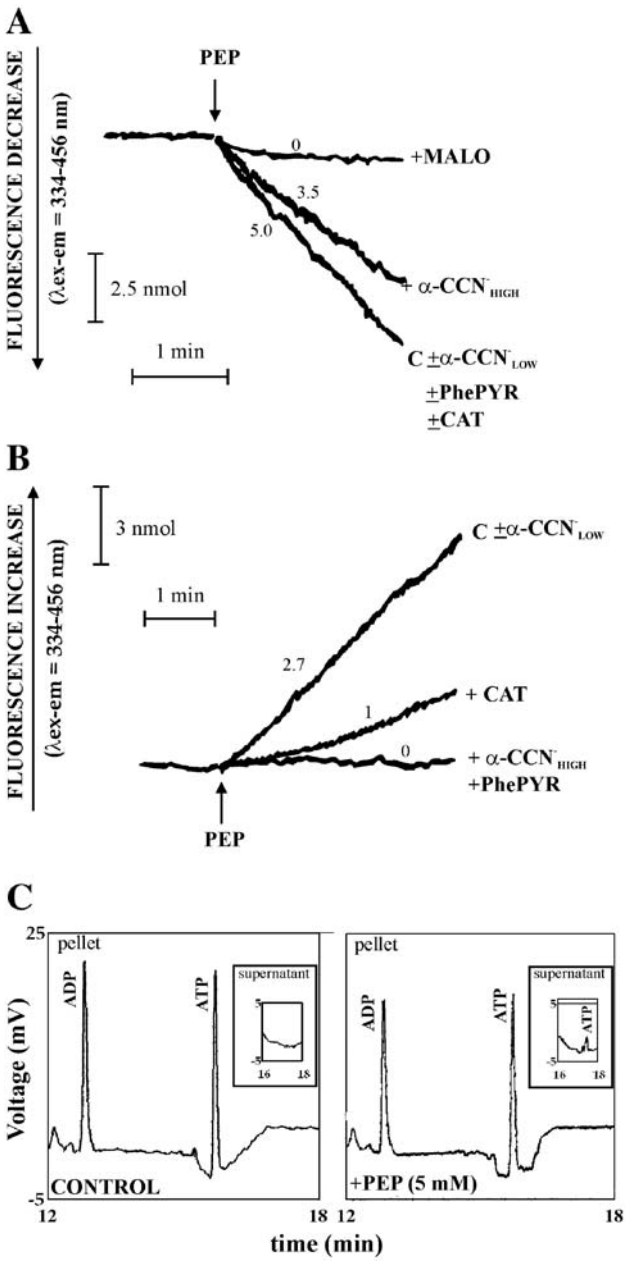

Fig. 5. Appearance of pyruvate and ATP induced by PEP addition to JAM and HPLC analysis of ADP and ATP levels after PEP addition to JAM. (A, B) JAM (1 mg protein) were suspended at 25 °C in 2 mL of standard medium in the presence of either (A) the P.D.S. (20 μM NADH plus 1 e.u. L-LDH) plus ROT (2 μg), EGTA (10 mM) and diphenyleneiodonium (DPI, 5 μM), or (B) the ATP D.S. plus Ap5A (0.1 mM) and succinate (5 mM). At the arrow PEP (5 mM) was added in the absence (C) or presence of the following inhibitors (added 1 min before the substrate): MALO (10 mM), phenylpyruvate (PhePYR, 10 mM), α-cyano-4-hydroxycinnamate (α-CCN^-_{LOW}, 25 μM), α-CCN^-_{HIGH}, (1 mM) or carboxyatractyloside (CAT, 10 μM). Externally added pyridine nucleotide oxidation or reduction was followed fluorimetrically (λ_{exc}=334 nm; λ_{em}=456 nm) as a function of time. The numbers give the rate of fluorescence changes measured as tangents to the initial part of the progress curves and expressed as nmol NADH oxidized ($NADP^+$ reduced)/min×mg mitochondrial protein. (C) JAM (1 mg protein) were incubated at 25 °C in 1 mL of standard medium. The amounts of ADP and of ATP, were measured in neutralized perchloric acid extracts of both the pellet and supernatant (insets) fractions of JAM, as described in Materials and methods. Where indicated, PEP (5 mM) was pre-incubated with JAM.

appearance of ATP outside mitochondria (ATP_{OUT}) with a $ATP_{OUT}/\Delta(ADP_{IN}+ATP_{IN})$ ratio close to 1. Even though the endogenous nucleotide content of the JAM preparations were significantly different, a ratio close to 1 was found in three different experiments (Table 1). Notice that HPLC allows for measurements of ATP concentrations lower than those that can be monitored fluorimetrically.

Both to ascertain that pyruvate or ATP efflux due to externally added PEP occurs in a carrier-mediated manner and to rule out the involvement of the pyruvate and ADP/ATP carriers in the transport, we checked the sensitivity of the PEP-dependent metabolite efflux to different compounds that cannot enter mitochondria (Fig. 5A, B). In particular, the PEP-dependent pyruvate efflux does not occur via the pyruvate carrier since it was not inhibited by 25 μM α-CCN– (αCCN^-_{LOW}), a potent inhibitor of the monocarboxylate carrier [34], which proved to completely block pyruvate uptake by JAM via the monocarboxylate carrier, monitored fluorimetrically as in [1] (not shown). That PEP dependent ATP efflux occurs via the ADP/ATP carrier is ruled out since it was inhibited by 1 mM α-CCN (αCCN_{HIGH}) which had no effect on the ADP/ATP carrier measured fluorimetrically as reported in Materials and methods (not shown). Moreover, either phenylpyruvate (PhePYR; 10 mM) or carboxyatractyloside (CAT; 10 μM), proved to inhibit ATP but not pyruvate efflux due to PEP addition to JAM, thus showing that PEP/pyruvate and PEP/ATP exchanges occur in a different manner (Fig. 5A, B).

In the same experiment we found that BEMA (10 mM), which inhibits both swelling and PEP uptake, was ineffective in inhibiting either pyruvate or ATP efflux, whereas BTA (1 mM) completely inhibited both of them (not shown). The differences between the inhibition profiles show that pyruvate and ATP appearance outside JAM in exchange with PEP take place via two different carriers, themselves separate from that mediating PEP uptake.

To confirm that the rates of externally added NADH oxidation/$NADP^+$ reduction, due to PEP addition in the presence of P.D.S. and ATP D.S. respectively, mirror that of pyruvate and ATP transport, control flux analysis [34] was carried out as above, by investigating the dependence of the rate of either fluorescence decrease or increase on increasing α-CCN^- (Fig. 6A, a) or CAT (Fig. 6B, a) concentrations, respectively, at 0.5 and 5 mM PEP. α-CCN^- proved to be a competitive inhibitor of the rate of pyruvate appearance with K_i value equal to 0.7 mM; CAT proved to inhibit ATP appearance in a non-competitive manner with K_i value equal to 6 μM. To confirm that ATP efflux does not occur via the ADP/ATP carrier, we showed that CAT is a competitive inhibitor of the ADP/ATP carrier, with a K_i value equal to 6 μM, (inset of Fig. 6B, a). Control flux analysis carried out as above shows that the rate of NADH oxidation/$NADP^+$ reduction reflects the rate of the PEP/pyruvate and PEP/ATP exchange, respectively.

The dependence of the rate of PEP/pyruvate and PEP/ATP antiports on increasing PEP concentrations was measured and results analyzed by means of a Michaelis–Menten plot (Fig. 6A, b; B, b). In both cases saturation kinetics were found with

Table 1
The changes of both mitochondrial and extramitochondrial ADP and ATP amount due to the addition of PEP to JAM as investigated by HPLC

	ADP (nmol/mg prot)						ATP (nmol/mg prot)					
	Experiment 1		Experiment 2		Experiment 3		Experiment 1		Experiment 2		Experiment 3	
	pellet	supernatant	pellet	supernatant	pellet	supernatant	pellet	supernatant	pellet	supernatant	pellet	supernatant
CONTROL	1.00±0.04	0.00	1.52±0.04	0.00	1.24±0.04	0.00	0.76±0.03	0.00	0.98±0.04	0.00	0.84±0.04	0.00
+PEP	0.77±0.02	0.00	0.97±0.04	0.00	0.83±0.04	0.00	0.63±0.03	0.32±0.01	0.79±0.03	0.67±0.02	0.71±0.03	0.45±0.02
+PEP +OLIGO	0.78±0.03	0.00	1.12±0.04	0.00	0.96±0.03	0.00	0.61±0.02	0.10±0.01	1.00±0.04	0.35±0.04	0.65±0.04	0.29±0.02

JAM (1 mg protein) were incubated at 25 °C in 1 mL of standard medium. Where indicated, PEP (5 mM) was added to JAM either in the absence or presence of OLIGO (2.5 μg/mL), as described in Materials and methods. The amounts of ADP and of ATP were measured in neutralized perchloric acid extracts of both the pellet and the supernatant fractions. The data reported are means (±SD) of three independent measurements carried out in each experiment.

K_m values equal to 200 μM and 500 μM and V_{max} values equal to 5 and 3 nmol/min × mg mitochondrial protein, respectively. In three experiments, carried out with different preparations, the mean K_m values were found to be 200±10 and 500±20 μM, whereas the mean V_{max} values were found to be 5±0.3 and 3±0.3 nmol/min × mg mitochondrial protein, for the PEP/pyruvate and PEP/ATP antiporters, respectively. As a control, the ADP/ATP exchange rate was measured in the same experiment at increasing ADP concentrations and the experimental data analyzed by means of a Michaelis–Menten plot (inset of Fig. 6B, b). K_m and V_{max} values of 1 μM and 10 nmol/min × mg mitochondrial protein, respectively, were found.

To gain further insight into the mechanism of PEP uptake by JAM as well as into the physiological role of the mitochondrial PEP metabolism, the capability of PEP to cause the efflux of several compounds other than pyruvate and ATP, was checked. In initial investigations, the appearance of malate, oxaloacetate (OAA) and citrate outside mitochondria was monitored photometrically or fluorimetrically by using specific metabolite detecting systems (see Materials and methods) (Fig. 7). The concentration of OAA, citrate and malate outside mitochondria were negligible since no change in the NAD(P)H fluorescence or absorbance was found in the presence of O.D.S., C.D.S. and M.D.S., respectively. As a result of 5 mM PEP addition, OAA (Fig. 7A), citrate (Fig. 7B) but not malate (Fig. 7C) appearance was found as shown by the decrease of NADH fluorescence, in the case of OAA and citrate, and by the lack of increase of the NADPH absorbance in the case of malate. The rate of citrate efflux (4 nmol/min × mg protein) was obtained by subtracting the rate of OAA efflux previously measured (6 nmol/min × mg protein), from the rate found in the presence of C.D.S. (10 nmol/min × mg protein) (see Materials and methods). Phenylsuccinate (PheSUCC, 10 mM) and BTA (1 mM) were found to inhibit the appearance of oxaloacetate and citrate, respectively. Interestingly, BTA had no effect on OAA appearance rate, thus suggesting the involvement of two different transport processes for OAA and citrate efflux (Fig. 7A, B). In a control experiment, the addition of succinate (5 mM) to JAM incubated with M.D.S., produced a fast increase in NADPH absorbance due to malate efflux in the extramitochondrial phase in exchange with succinate, via the dicarboxylate carrier [1] (Fig. 7C).

4. Discussion

In this paper we show for the first time that PEP can be transported into plant mitochondria, in particular those from Jerusalem artichoke tubers, and be metabolized therein. The sequence of events involved in PEP metabolism includes PEP uptake by mitochondria, pyruvate and ATP synthesis inside mitochondria due to the novel mitochondrial PK, oxidation of the intramitochondrial NAD(P)H due to the activation of the AOX, PEP/pyruvate and PEP/ATP antiports which are assumed to take place via two separate carriers distinct from the pyruvate and the ADP/ATP carriers. These points will be discussed separately below.

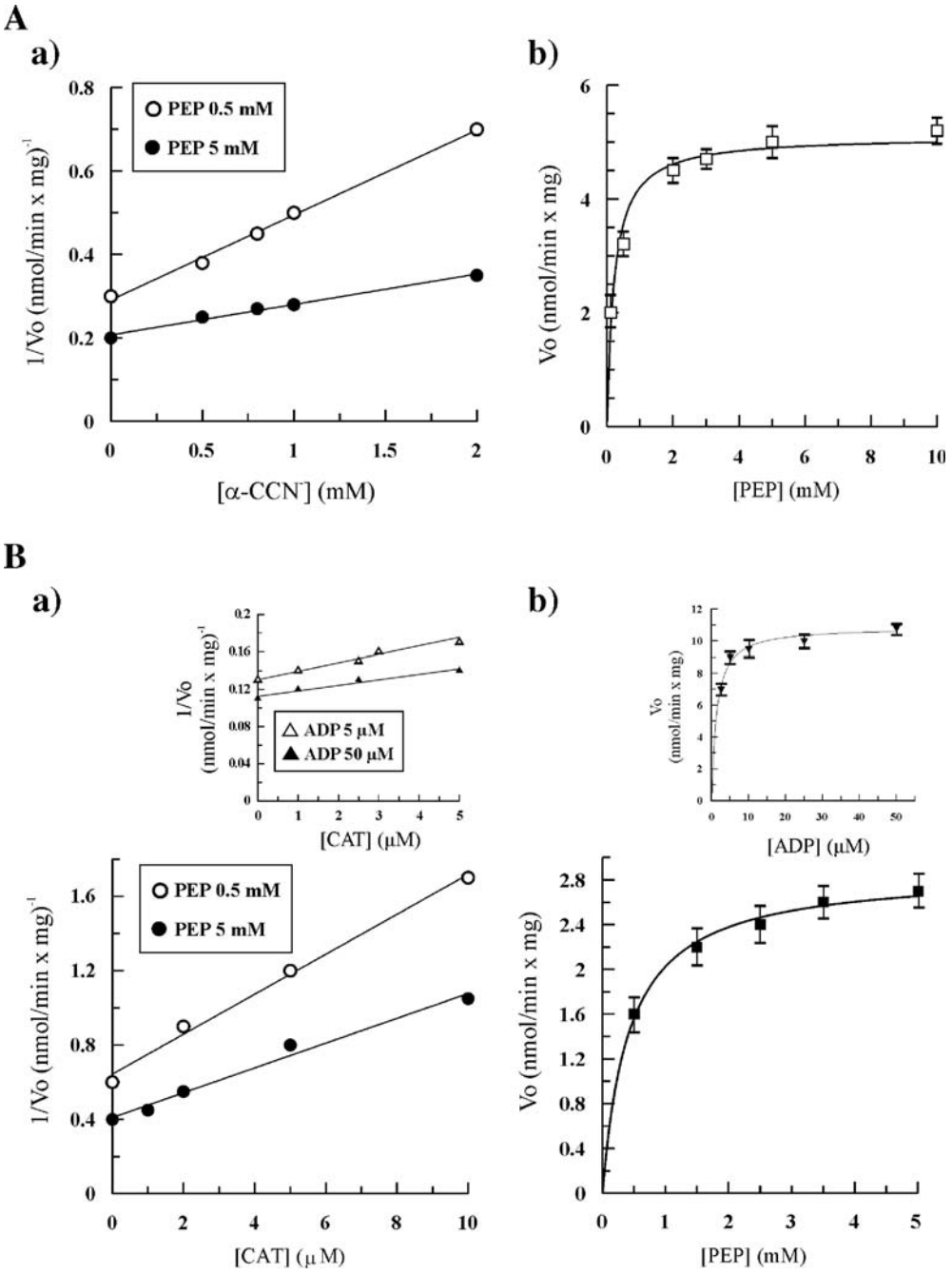

Fig. 6. Dixon plot of the inhibition by αCCN⁻ and CAT of the rate of pyruvate and ATP appearance due to externally added PEP. Dependence of PEP/pyruvate and PEP/ATP antiports on increasing PEP concentrations. JAM (1 mg protein) were incubated at 25 °C in 2 mL of standard medium. The rate of pyruvate (A) or ATP (B) appearance in the extramitochondrial phase was measured as described in Fig. 5. PEP (0.5 mM, or 5 mM) (A, a; B, a) or ADP (5 μM, or 50 μM) (inset of B, a) were added either in the absence or presence of α-CCN⁻ or CAT at the indicated concentrations. The rate (v_o), measured as the tangent to the initial part of the progress curve, is expressed as nmol NADH oxidized ($NADP^+$ reduced)/min × mg mitochondrial protein. Either PEP (A b; B, b) or ADP (inset of B, b) were added to JAM (1 mg protein) at the indicated concentrations and the rate of NADH oxidation (A, b)/$NADP^+$ reduction (B, b), reflecting the rate of pyruvate/ATP appearance, respectively, was measured as the tangent to the initial part of the progress curves and expressed as nmol/min × mg mitochondrial protein. Bars represent the mean (±SD) of three independent measurements.

To investigate PEP uptake by JAM, use was made of spectroscopic techniques under conditions in which mitochondrial metabolism is mostly active, thus allowing for monitoring mitochondrial reactions and the traffic of newly synthesized substrates across the mitochondrial membrane. JAM can take up PEP with net carbon uptake in a proton-compensated manner. This was first shown by the observed swelling in isotonic solutions of ammonium PEP which itself indicates that PEP uptake is proton-compensated (Scheme 1). Indication in favor of a carrier mediated transport derives from the inhibition of swelling due to BEMA which cannot enter JAM. Definitive confirmation is given by the occurrence of the hyperbolic

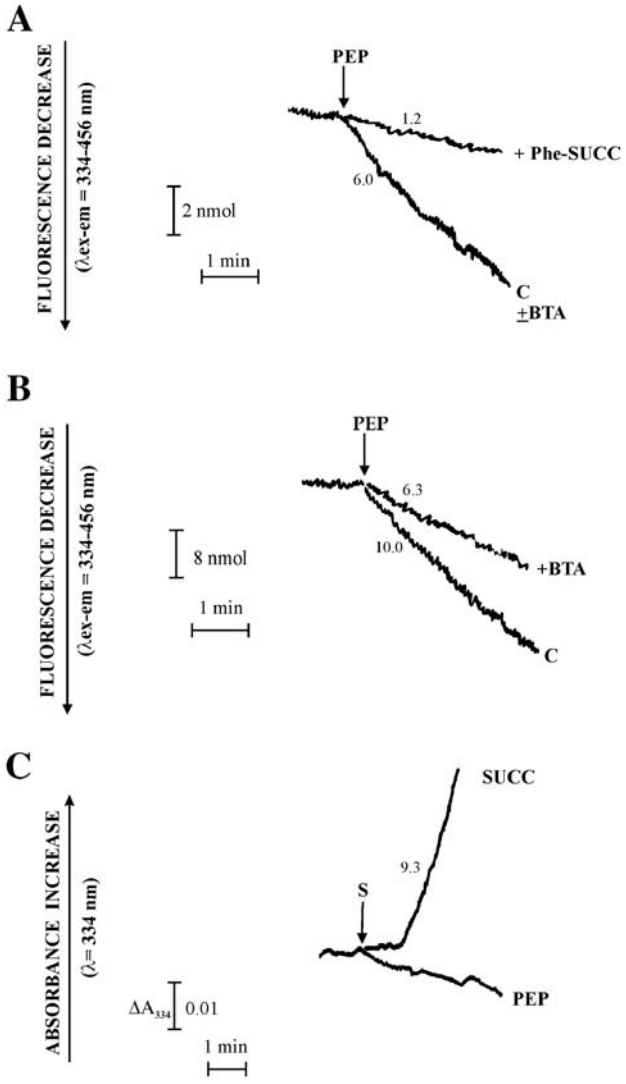

Fig. 7. Appearance of oxaloacetate and citrate in the extramitochondrial phase induced by the addition of PEP to JAM. JAM (1 mg protein) was suspended at 25 °C in 2 mL of standard medium in the presence of either (A) the oxaloacetate detecting system (O.D.S., 20 μM NADH plus 1 e.u. malate dehydrogenase), (B) the citrate detecting system (consisting of O.D.S. plus 1 e.u. citrate lyase, 1 mM ATP and 1 mM coenzyme A), or (C) the malate detecting system (200 μM $NADP^+$ plus 0.2 e.u. malic enzyme). In A and B rotenone (2 μg), EGTA (10 mM) and DPI (5 μM) were added to the mitochondrial suspension before the metabolite detecting system. At the arrow phosphoenolpyruvate (PEP, 5 mM) was added in the absence (C) or presence of phenylsuccinate (PheSUCC, 10 mM) or BTA (1 mM). In C, the substrate (S), *i.e.* PEP or succinate (SUCC), both 5 mM, was added at the arrow. Pyridine nucleotide oxidation was followed fluorimetrically as a function of time. The numbers give the rate of fluorescence decrease (λ_{exc}=334 nm; λ_{em}=456 nm) (A, B) or absorbance increase (λ=334 nm) (C) measured as tangents to the initial part of the progress curves and expressed as nmol NADH oxidized ($NADP^+$ reduced)/min × mg mitochondrial protein.

kinetics of the transport and by the inhibition studies as fluorimetrically investigated. Indeed, we have been forced to use a non-traditional approach in investigating PEP uptake. As opposed to the expected increase of NAD(P)H fluorescence due to the $NAD(P)^+$ reduction arising from the intramitochondrial metabolism of the newly synthesized pyruvate, as a result of PEP addition to JAM we observe intramitochondrial NAD(P)H oxidation due to the activation of AOX as shown by the capability of both Propyl-GALL and SHAM, AOX inhibitors, to inhibit this process (Fig. 4). Nonetheless, in spite of the four steps involved in this process, *i.e.* PEP uptake, the PK reaction, AOX activation by PEP and pyruvate with the consequent intramitochondrial NAD(P)H oxidation, we maintain that the decrease of fluorescence mirrors the transport step, its rate being the limiting step of the entire process, as shown by applying control strength criterion (Fig. 4C, b). Consistently, we have found that no inhibition in the rate of NAD(P)H oxidation takes place in a definite low concentration range of both Propyl-GALL and SHAM (Fig. 4C, a). Malonate which can completely inhibit PK activity (Fig. 1B, a), was ineffective on the rate of PEP-dependent NAD(P)H oxidation, showing that PEP itself is an AOX activator (Fig. 4B). Notice that the measured rate derives from the balance between the NAD(P)H producing and consuming reactions, as indicated by the increase of the oxidation rate observed in the presence of arsenite and cyanide, inhibitors of the pyruvate dehydrogenase complex and of the COX respectively.

The results that we have reported show the existence of a mitochondrial PK (see Fig. 1). Such a conclusion derives from the immunological analysis reported in Fig. 1A, confirmed by kinetic studies in which we show saturation characteristics for the reaction in solubilized JAM. In this case we avoid assaying PK routinely via L-LDH and NADH, since NADH at the used concentration, is rapidly oxidized by the external NAD(P)H dehydrogenase (inset to Fig. 1B, a). In contrast, the fluorimetric method used to monitor ATP appearance allows for the measurement at micromolar concentration of NADPH which is not oxidized by the external NAD(P)H dehydrogenase as already shown in [43] and as found in a control experiment carried out with JAM, not shown here. Since the putative PK activity can be assayed only in solubilized JAM, PK must be localized on the inner side of the mitochondrial inner membrane or in the matrix space. Moreover ATP synthesis measured via HPLC in the mitochondria incubated only with PEP in the absence of external ADP is not consistent with PK localization in the external compartments (Fig. 5C and Table 1).

The discovery of the mitochondrial PK, as derived from both immunological and functional studies, is consistent with the results we obtained from the TAIR (Arabidopsis Information Resource) gene search in which two matches correspond to PK isoforms predicted by Target P program to be located in mitochondria. Thus, at present we cannot rule out that the measured PK activity is due to two mitochondrial isoforms. Nonetheless, it/they is/are different from that/those investigated in the cytosolic fraction as shown by the different inhibition and pH profiles.

Discussion of the role of mitochondrial PK can only be speculative. Having established via HPLC that the intramitochondrial ADP amount decreases with no ADP found outside JAM (Table 1), we must assume that the mitochondrial PEP metabolism results in a decrease in the rate of the isocitrate dehydrogenase reaction, which is highly dependent on ADP

intramitochondrial concentration, and possibly of the citric cycle; on the other hand, we show additional AOX activation due to PEP itself (see Scheme 1), which promotes intramitochondrial NAD(P)H oxidation also in the presence of the PK inhibitor malonate. Thus it is proposed that PEP and pyruvate are together AOX activators, with PEP involved in the AOX puzzle (see [44]).

This paper gives a first indication in favor of the occurrence of two novel carriers: the PEP/pyruvate and PEP/ATP antiporters (Figs. 5 and 6). When studying both PEP/ATP and PEP/pyruvate exchanges, control flux analysis application (see [35]) showed that the measured changes in fluorescence mirror the rate of substrates transport (Fig. 6A, a; B, a). Thus if the situation *in vivo* is similar to that *in vitro*, then the metabolism of PEP is regulated by transport processes. Moreover, we show that PEP antiporters differ from each other, from the PEP symporter and from the pyruvate and ADP/ATP carriers on the basis of the different sensitivity to certain non-penetrant compounds.

At present, the role of effluxed pyruvate in the cytoplasm remains unclear; the possibility should be considered that it may participate in the biosynthesis of storage proteins (see Scheme 1). The effluxed ATP is assumed to enter the cytosolic pool, thus contributing to energy metabolism.

PEP might play a major role in directing carbohydrate towards plastidic fatty acid biosynthesis versus the mitochondrial ATP production and organic acid required for aminoacid inter-conversion in support of storage protein biosynthesis [10]. This paper opens new scenarios to PEP plant metabolism. Indeed, if we assume that the cytosolic PEP concentration is in the millimolar range as reported in mesophyll cells of spinach [45] then the K_m values for PEP uptake are consistent with the physiological occurrence of PEP mitochondrial uptake and metabolism.

We suggest that, as a result of the PEP metabolism via the putative mitochondrial PK, reduction in isocitrate dehydrogenase activity could occur (see above), with consequent increase of matrix citrate concentration which could determine its efflux outside mitochondria. Consistently, in initial experiments we have found that JAM incubated with PEP can export citrate and oxaloacetate to the extramitochondrial phase (Fig. 7) thus also providing a novel pathway accounting for ammonia incorporation and fatty acid synthesis (see Scheme 1).

Acknowledgements

The authors thank Prof Shawn Doonan for his critical reading. The skill cooperation of Dr G. Chieppa in the immunological experiments is gratefully acknowledged. This work was partially financed by Fondi di Ricerca di Ateneo del Molise and FIRB RBNE03B8KK_003 (to S.P.).

References

[1] A. Atlante, L. de Bari, D. Valenti, R. Pizzuto, G. Paventi, S. Passarella, Transport and metabolism of D-lactate in Jerusalem artichoke mitochondria, Biochim. Biophys. Acta Bioenerg. 1708 (2005) 13–22.

[2] L. de Bari, D. Valenti, R. Pizzuto, G. Paventi, A. Atlante, S. Passarella, Jerusalem artichoke mitochondria can export reducing equivalents in the form of malate as a result of D-lactate uptake and metabolism, Biochem. Biophys. Res. Commun. 335 (2005) 1224–1230.

[3] W.C. Plaxton, The organization and regulation of plant glycolysis, Annu. Rev. Plant Physiol., Plant Mol. Biol. 47 (1996) 185–214.

[4] F.E. Podesta', W.C. Plaxton, Kinetic and regulatory properties of cytosolic pyruvate kinase from germinating castor oil seeds, Biochem. J. 279 (1991) 495–501.

[5] F.E. Podesta', W.C. Plaxton, Activation of cytosolic pyruvate kinase by polyethylene glycol, Plant Physiol. 103 (1993) 285–288.

[6] F.E. Podesta', W.C. Plaxton, Regulation of cytosolic carbon metabolism in germinating *Ricinus communis* cotyledons: II. Properties of phosphoenolpyruvate carboxylase and cytosolic pyruvate kinase associated with the regulation of glycolysis and nitrogen assimilation, Planta 194 (1994) 381–387.

[7] Z. Hu, C. Plaxton, Purification and characterization of cytosolic pyruvate kinase from leaves of the castor oil plant, Arch. Biochem. Biophys. 333 (1996) 298–307.

[8] C.R. Smith, V.L. Knowles, W.C. Plaxton, Purification and characterization of cytosolic pyruvate kinase from *Brassica napus* (rapeseed) suspension cell cultures. Implications for the integration of glycolysis with nitrogen assimilation, Eur. J. Biochem. 267 (2000) 4477–4485.

[9] W.L. Turner, W.C. Plaxton, Purification and characterization of cytosolic pyruvate kinase from banana fruit, Biochem. J. 352 (2000) 875–882.

[10] W.L. Turner, V.L. Knowles, W.C. Plaxton, Cytosolic pyruvate kinase: subunit composition, activity, and amount in developing castor and soybean seeds, and biochemical characterization of the purified castor seed enzyme, Planta 222 (2005) 1051–1062.

[11] S.A. McCloud, R.G. Smith, K.A. Schuller, Partial purification and characterization of pyruvate kinase from the plant fraction of soybean root nodules, Physiol. Plant 111 (2001) 283–290.

[12] I.M. Juszczuk, A.M. Rychter, Pyruvate accumulation during phosphate deficiency stress of bean roots, Plant Physiol. Biochem. 40 (2002) 783–788.

[13] D.A. Day, J.B. Hanson, Pyruvate and malate transport and oxidation in corn mitochondria, Plant Physiol. 59 (1977) 630–635.

[14] A.S. Hill, J.H. Bryce, C.J. Leaver, Pyruvate metabolism in mitochondria from cucumber cotyledons during early seedling development, J. Exp. Bot. 45 (1994) 1489–1491.

[15] M.W. Fowler, Role of the malic enzyme reaction in plant roots, utilization of [2,3-^{14}C]malate, [4-^{14}C]malate, and [1-^{14}C]pyruvate by pea root apices and measurement of enzyme activity, Biochem. Biophys. Acta 372 (1974) 245–254.

[16] J.T. Wiskich, Control of the Krebs cycle, in: D.D. Davies (Ed.), The Biochemistry of Plants, vol. 2, Academic Press, New York, 1980, pp. 243–278.

[17] J.H. Bryce, T. ap Rees, Rapid decarboxylation of the products of dark fixation of CO_2 in roots of *Pisum* and *Plantago*, Phytochemistry 24 (1985) 1635–1638.

[18] P. Giege, J.L. Heazlewood, U. Roessner-Tunali, A.H. Millar, A.R. Fernie, C.J. Leaver, L.J. Sweetlove, Enzymes of glycolysis are functionally associated with the mitochondrion in Arabidopsis cells, Plant Cell 15 (2003) 2140–2151.

[19] A.C. Liden, I.M. Moller, Purification, characterization and storage of mitochondria from Jerusalem artichoke tubers, Physiol. Plant 72 (1988) 265–270.

[20] M. Neuburger, E.P. Journet, R. Bligny, J.P. Carde, R. Douce, Purification of plant mitochondria by isopycnic centrifugation in density gradients of percoll, Arch. Biochem. Biophys. 217 (1982) 312–323.

[21] M.L. Pallotta, D. Valenti, M. Iacovino, S. Passarella, Two separate pathways for D-lactate oxidation by *Saccharomyces cerevisiae* mitochondria which differ in energy production carrier involvement, Biochim. Biophys. Acta 1608 (2004) 104–113.

[22] G. Paventi, D. Pastore, A. Bobba, R. Pizzuto, S. Di Pede, S. Passarella, Plant uncoupling protein in mitochondria from aged-dehydrated slices of Jerusalem artichoke tubers becomes sensitive to superoxide and to hydrogen peroxide without increase in protein level, Biochimie 88 (2006) 179–188.

[23] G.W. Lohr, H.D. Waller, Glucose-6-phosphate dehydrogenase, in: H.U. Bergmeyer (Ed.), Methods of Enzymatic Analysis, 1963, pp. 744–751.
[24] A. Atlante, T.M. Seccia, P. Pierro, V. Vulpis, E. Marra, A. Pirrelli, S. Passarella, ATP synthesis and export in heart left ventricle mitochondria from spontaneously hypertensive rat, Int. J. Mol. Med. 1 (1998) 709–716.
[25] U.K. Laemmli, Cleavage of structural proteins during the assembly of the head of bacteriophage T4, Nature 227 (1970) 680–685.
[26] S. Passarella, A. Ostuni, A. Atlante, E. Quagliariello, Increase in the ADP/ATP exchange in rat liver mitochondria irradiated in vitro by helium-neon laser, Biochem. Biophys. Res. Commun. 156 (1988) 978–986.
[27] A. Atlante, L. de Bari, A. Bobba, E. Marra, P. Calissano, S. Passarella, Cytochrome *c*, released from cerebellar granule cells undergoing apoptosis or excitotoxic death, can generate protonmotive force and drive ATP synthesis in isolated mitochondria, J. Neurochem. 86 (2003) 591–604.
[28] S. Passarella, A. Atlante, E. Quagliariello, Oxaloacetate permeation in rat kidney mitochondria: pyruvate/oxaloacetate and malate/oxaloacetate translocators, Biochem. Biophys. Res. Commun. 129 (1985) 1–10.
[29] A. Atlante, S. Passarella, G.M. Minervini, E. Quagliariello, Glutamine transport in normal and acidotic rat kidney mitochondria, Arch. Biochem. Biophys. 315 (1994) 369–381.
[30] A. Atlante, S. Passarella, P. Pierro, C. Di Martino, E. Quagliariello, The mechanism of proline/glutamate antiport in rat kidney mitochondria. Energy dependence and glutamate-carrier involvement, Eur. J. Biochem. 241 (1996) 171–177.
[31] G.E. Lienhard, I.I. Secemski, P1,P5-Di(adenosine-5′)pentaphosphate, a potent multisubstrate inhibitor of adenylate kinase, J. Biol. Chem. 248 (1973) 1121–1123.
[32] D. Pastore, C. Di Martino, G. Bosco, S. Passarella, Stimulation of ATP synthesis via oxidative phosphorylation in wheat mitochondria irradiated with helium-neon laser, Biochem. Mol. Biol. Int. 39 (1996) 149–157.
[33] A. Atlante, S. Giannattasio, A. Bobba, S. Gagliardi, V. Petragallo, P. Calissano, E. Marra, S. Passarella, An increase in the ATP levels occurs in cerebellar granule cells en route to apoptosis in which ATP derives from both oxidative phosphorylation and anaerobic glycolysis, Biochim. Biophys. Acta 1708 (2005) 50–62.
[34] A.P. Halestrap, R.D. Scottand, A.P. Thomas, Mitochondrial pyruvate transport and its hormonal regulation, Int. J. Biochem. 11 (1980) 97–105.
[35] S. Passarella, A. Atlante, D. Valenti, L. de Bari, The role of mitochondrial transport in energy metabolism, Mitochondrion 2 (2003) 319–343.
[36] L. de Bari, A. Atlante, N. Guaragnella, G. Principato, S. Passarella, D-lactate transport and metabolism in rat liver mitochondria, Biochem. J. 365 (2002) 391–403.
[37] M. Ribas-Carbo, A. Joseph, B.D. Yakir, L. Giles, S.A. Robinson, A.M. Lennon, J.N. Siedow, Electron partitioning between the cytochrome and alternative pathways in plant mitochondria, Plant Physiol. 109 (1995) 829–837.
[38] G.C. Vanlerberghe, D.A. Day, J.T. Wiskich, A.E. Vanlerberghe, L. McIntosh, Alternative oxidase activity in tobacco leaf mitochondria. Dependence on tricarboxylic acid cycle-mediated redox regulation and pyruvate activation, Plant Physiol. 109 (1995) 353–361.
[39] A.H. Millar, M.H.N. Hoefnagel, D.A. Day, J.T. Wiskich, Specificity of the organic acid activation on the alternative oxidase in plant mitochondria, Plant Physiol. 111 (1996) 613–618.
[40] G.R. Schonbaum, W.D. Bonner, B.T. Storey, J.T. Bahr, Specific inhibition of the cyanide-insensitive respiratory pathway in plant mitochondria by hydroxamic acids, Plant Physiol. 47 (1971) 124–128.
[41] J.N. Siedow, M.E. Girvin, Alternative respiratory pathway. Its role in seed respiration and its inhibition by propyl gallate, Plant Physiol. 65 (1980) 669–674.
[42] D. Pastore, D. Trono, M.N. Laus, N. Di Fonzo, S. Passarella, Alternative oxidase in Durum Wheat mitochondria. Activation by pyruvate, hydroxypyruvate and glyoxylate and physiological role, Plant Cell Physiol. 42 (2001) 1373–1382.
[43] D. Pastore, S. Di Pede, S. Passarella, Isolated durum wheat and potato cell mitochondria oxidize externally added NADH mostly via the malate/oxaloacetate shuttle with a rate that depends on the carrier-mediated transport, Plant Physiol. 133 (2003) 2029–2039.
[44] A.L. Moore, J.N. Siedow, The regulation and nature of the cyanide-resistant alternative oxidase of plant mitochondria, Biochim. Biophys. Acta 1059 (1991) 121–140.
[45] A.S. Raghavendra, S. Reumann, H.W. Heldt, Participation of mitochondrial metabolism in photorespiration. Reconstituted system of peroxisomes and mitochondria from spinach leaves, Plant Physiol. 116 (1998) 1333–1337.